hydrogen

MDPI

Article

Polarization and Forward Scattering Effects in Low Energy Positron Collisions with H_2

Wagner Tenfen [1,*], Josiney de Souza Glória [1], Sarah Esther da Silva Saab [1], Eliton Popovicz Seidel [2,3] and Felipe Arretche [3]

[1] Physics Department, Universidade Federal de Pelotas, Pelotas 96010-610, Rio Grande do Sul, Brazil
[2] Division of Computational Chemical Physics, Faculty of Applied Physics and Mathematics, Gdańsk University of Technology, 80-233 Gdańsk, Poland
[3] Physics Department, Universidade Federal de Santa Catarina, Florianópolis 88040-900, Santa Catarina, Brazil
* Correspondence: wtenfen@ufpel.edu.br

Abstract: Positron physical-chemistry has been one important focus of scientific investigation of the last decades, however their low energy scattering by atoms and molecules still offers many questions to be answered, as the low angle scattering effects on the measured cross sections and how the degree of target polarization manifest in the comparison between theoretical and experimental results. In this work, we investigate low energy positron collisions by H_2 molecules, with particular attention to the convergence of the polarization contribution on the scattering potential. The interaction between positron and molecule was represented by a model potential conceived from the composition of a free electron gas correlation term with an asymptotic polarization potential, obtained from perturbation theory. In particular, we investigated how polarization effects beyond the second order perturbation affect the scattering observables. Our results show that the model which includes up to the quadrupole polarization contribution presents better agreement to the recent experimental data when corrected for forward scattering effects, since they were measured from a transmission beam technique. The angular distributions were also examined through the comparison between our results to the folded differential cross sections measurements available in the literature. We propose a simple correction scheme to the experimental folded differential cross sections for energies below 1 eV which then, as we argue, favorably compares to the quadrupole polarization model. Finally, the comparison between our phase shifts and scattering lengths with recent full many body ab initio results that explicitly include virtual positronium effects suggests that these are intrisically included in the adopted model correlation potential.

Keywords: molecular hydrogen; positron; elastic scattering; polarization

Academic Editors: Katsuaki Tanabe and Rui C. Vilão

Received: 19 October 2024
Revised: 4 December 2024
Accepted: 7 January 2025
Published: 10 January 2025

Citation: Tenfen, W.; Glória, J.d.S.; Saab, S.E.d.S.; Popovicz Seidel, E.; Arretche, F. Polarization and Forward Scattering Effects in Low Energy Positron Collisions with H_2. *Hydrogen* **2025**, *6*, 2. https://doi.org/10.3390/hydrogen6010002

1. Introduction

Positron scattering by atoms and molecules is widely recognized as a difficult problem. Even though there are many possible applications, as in material sciences [1–3], medicine [4–6], and astrophysics [7–10], to cite a few, the fundamental aspects of the interaction between a positron and an atomic or molecular target is still under discussion. Differently from the electron scattering case, the correlation and polarization effects of the positron over the target must be carefully described, since the absence of an exchange interaction makes the delicate balance between the electrostatic and distortion effects determinant over the scattering cross sections. In particular, virtual positronium formation is a correlation effect whose role in scattering dynamics is still to be better understood [11–13].

For the hydrogen molecule the scenario is not different. Many experimental and theoretical studies for the scattering of low energy positrons by this molecule are available in the literature [13–30] . Even for the elastic scattering, the agreement between theory and experiment is, still today, only marginal. One source of such disagreement is the limited angular resolution of transmission based spectrometers, where the positrons elastically scattered below a characteristic angle are counted as unscattered, undervaluating the measured total cross section (TCS) [31–33]. This discrepancy can be corrected if one has access to reliable differential cross sections, measured or calculated [34]. However, such experimental data is very scarce, while on the theoretical side, it is very difficult to choose between the various theoretical approaches the one that describes the phenomenon appropriately. While there are theoretical approaches more convincing than others, a systematic theoretical description of the experimental positron scattering data is still an ongoing scientific effort, and constitutes an important open problem.

Among the many theoretical approaches for positron scattering with molecules, two methodologies are predominant: the full ab initio many body and the model potential approaches. Each of those methods have their own merits. While it is desirable to obtain a many body wave function for the positron molecule system, calculated with little approximations as possible, the model potential approaches generally are based on scattering potentials, which are easier to interpret and to adjust in order to better compare the theoretical cross sections to the experimental data [35].

Specifically in the positron scattering with H_2 problem, we have plenty (but not nearly sufficient) theoretical and experimental data. From the theoretical perspective, there are ab initio results [13,19,21,23,26,28–30,36,37] and a number of model potential approximations [20,22,24,25,27]. The agreement of the theories with the experimental data seems to evolve in time, as a function of the available measurements. This is, the publication of new experimental data has the potential of changing the level of agreement among theory and experiment, as happened for the positron energies between 1 eV to approximatelly 10 eV when Zecca et al. published their experiment results [17]. It is noteworthy that there were no data for incident positron energies below 1 eV until then, and still today their results are the only available for energies below 0.5 eV, a critical region for comparison with theoretical results.

The experimental data of Zecca et al. [17] was obtained with a transmission based positron spectrometer, which is prone to underestimate the scattering cross sections as the elastically scattered positrons below a certain angle will be counted as unscattered, undervaluating the measurements as stated above. These cross sections were corrected for the low angle scattering effects with a full ab initio treatment [29], however the experimental data was not enhanced as much as expected, due to correlation and polarization effects that are not fully included as indicated by the comparison of their folded differential cross sections (FDCS) with available measurements. The comparison between theory and measurements becomes even more interesting with a more recent many body calculation [13], which supposedly included full correlation effects, resulting in significantly higher cross sections. Within this scenario, we propose to study positron scattering by H_2 from a model potential approach, in order to understand how the inclusion of these effects influences the calculated cross sections and the forward scattering corrections for the available experimental data. Following our previous works [38,39], we will include the correlation effects with the PCOP (positron correlation polarization) approach, changing the polarization term to include not only the second order perturbation theory polarizations, but also the relevant hyperpolarizabilities, and study the effects of these on the calculated integral and differential cross sections.

2. Theoretical Approach

The scattering model adopted in this study is given by the static plus correlation polarization (SCP) approximation

$$V(\vec{r}) = V_{st}(\vec{r}) + V_{cp}(\vec{r}), \tag{1}$$

where $V_{st}(\vec{r})$ is the electrostatic interaction between the positron and the H_2 molecule, and $V_{cp}(\vec{r})$ is the correlation polarization term, which is responsible to model the electron cloud distortion due to the presence of a positron near the molecular field.

The electrostatic term is given by the standard expression

$$V_{st}(\vec{r}) = -\sum_i \int \frac{\phi_i^*(\vec{r}_i)\phi_i(\vec{r}_i)}{|\vec{r}_i - \vec{r}|} d\vec{r}_i + \sum_j \frac{Z_j}{|\vec{R}_j - \vec{r}|}, \tag{2}$$

where $\vec{r}_i$ and $\vec{R}_j$ are the spatial coordinates of the i-th electron and j-th nucleus. A reasonable representation of the occupied orbitals $\phi_i(\vec{r}_i)$ in the given molecular state (the ground state in this study) is necessary in order to correctly describe the positron-electron interaction. It is well known that a Hartree-Fock (HF) representation of the molecular orbitals is sufficient for this end. This is always true in a model potential approach, because the electronic correlation effects can be considered through an external potential. It is more convenient to determine the coefficients from a potential expansion in a given spherical basis, which is known as a single center expansion [40]. So, we are interested in the calculation of the coefficients $V_{lm}(r)$ from

$$V_{st}(\vec{r}) = \sum_{lm} V_{lm}(r) Y_{lm}(\theta, \varphi), \tag{3}$$

where $\{r, \theta, \varphi\}$ are the spherical coordinates of the positron. Outside the electronic cloud, i.e., $r > r_i$ for every electron, the expansion coefficient can be related to the electrostatic moments of the molecule [41]. With this, we consider that the electronic wave function is well represented if the electrostatic moments of the molecule compare reasonably with the HF values from the literature.

For the correlation and polarization term we adopt the prescription of Jain and Gianturco [42]

$$V_{cp}(\vec{r}) = \begin{cases} V_{corr}(\vec{r}), & r \leq r_{cut} \\ V_{pol}(\vec{r}), & r > r_{cut} \end{cases} \tag{4}$$

where $V_{corr}(\vec{r})$ is the model potential for the correlation interaction and $V_{pol}(\vec{r})$ is the expression for the polarization obtained from perturbation theory [41,43], and the cut radius r_{cut} is the radial coordinate where the correlation and polarization functions cross each other for the first time. This matching scheme was originally proposed by O'Connell and Lane in the context of electron scattering [44]. They argued that this matching scheme do not have any physical meaning, being justified only by the adequacy of the resulting phase shifts. However, we have observed that this cut radius is somewhat related to the range of the electronic cloud [45], so the correlation effects that take place in the peripheral region of the molecule happens around this point. This is the case of the virtual positronium formation, for instance.

For the short range term of the correlation polarization potential it is necessary to adopt a model interaction. In this study we employed the correlation function derived by Jain and Gianturco [42], which is based on the correlation energy of a positron within a homogeneous electron gas as determined by Boroński and Nieminen [46]. The energy functional derived by them should take into account every effect of a positron immersed in a free electron gas, including the distortion of the electron density due to the formation of virtual positronium.

While this local density approximation is very useful to determine an interaction potential, other effects due to the inhomogeneity of the electron density in the real system will be absent from the model. The correlation energy is then parameterized in terms of the radius of a unit charge corresponding to the undisturbed molecular electron density

$$r_s = \sqrt[3]{\frac{3}{4\pi\rho(\vec{r})}}, \tag{5}$$

and can be written as

$$V_{corr}(\vec{r}) = \frac{1}{2}\begin{cases} \frac{-1.82}{\sqrt{r_s}} + (0.051\ln(r_s) - 0.115)\ln(r_s) + 1.167, & r_s \leq 0.302 \\ -0.92305 - \frac{0.09098}{r_s^2}, & 0.302 \leq r_s \leq 0.56. \\ -\frac{8.7674 r_s}{(r_s+2.5)^3} + \frac{-13.151+0.9552 r_s}{(r_s+2.5)^2} + \frac{2.8655}{(r_s+2.5)} - 0.6298, & 0.56 \leq r_s \leq 8.0 \end{cases} \tag{6}$$

For the polarization potential, we adopt the standard expression given by perturbation theory, as stated previously. However, it should be noted that since this potential curve is obtained from a perturbative series, one must add sufficient terms in order to guarantee its convergence. Recently, we observed that the scattering potential of small molecules only converges when we add up to the second hyperpolarizability term [38]. In order to study the convergence of the scattering potential with the polarization perturbative series, we include successively the terms corresponding to the dipole polarizability (α_D), the quadrupole polarizability (α_Q), the first mixed dipole quadrupole hyperpolarizability (B) and the second dipole hyperpolarizability (γ), so the full polarization potential reads

$$V_{pol}(\vec{r}) = -\frac{\alpha_0}{2r^4} - \frac{\alpha_2}{2r^4}P_2(\cos\theta) - \frac{\alpha_Q}{2r^6} + \frac{B}{2r^7} - \frac{\gamma}{24r^8}, \tag{7}$$

where α_0 and α_2 are the spherical and the anisotropic components of the dipole polarizability. For small molecules, all of the other terms of the spherical component of the potential are small compared to these ones, leaving future corrections to its anisotropic component. It is expected that the anisotropy in the polarization potential will influence (enhance) the cross sections for energies higher than 1 eV. Following our previous studies, we will name the successive scattering potentials given by the inclusion of the terms in Equation (7) as PD (up to α_D terms), PQ (up to α_Q), PB (up to B) and PG (up to γ).

The spherical term of the scattering potential ($V_0 = V_{00}Y_{00}$) for positron collisions with H_2 is presented in Figure 1. It is noticeable that the scattering potential only converges among PB and PG approaches, which means that the long range scattering potential can only be considered as complete in the PG approach. Now, if the electrostatic interaction is well described, which generally is the case, any criticism left to this approach should be directed towards the adequacy of adopting a correlation scheme designed for a homogeneous electron gas to describe the distortion of molecular orbitals by the presence of a positron. This is of fundamental importance in this approach, since it is the magnitude of the correlation potential in the peripheral region of the molecule that will define the value of r_{cut}, and hence strongly influence the scattering potential and the related cross sections. In Table 1 we provide the values for r_{cut} obtained in the different adopted approaches. We note that the values obtained for the approximations PQ, PB and PG are consistent with the longitudinal van der Waals radius for H_2 from Batsanov [47], which equals to $R_{vdW} = 2.87$ a.u.

Table 1. Values for the cut radius obtained in the different polarization approximations. Note that these values are close to the longitudinal $R_{vdW} = 2.87$ a.u. for PQ, PB and PG approaches.

Model	r_{cut} (a.u.)
PD	2.39
PQ	2.66
PB	2.90
PG	2.96

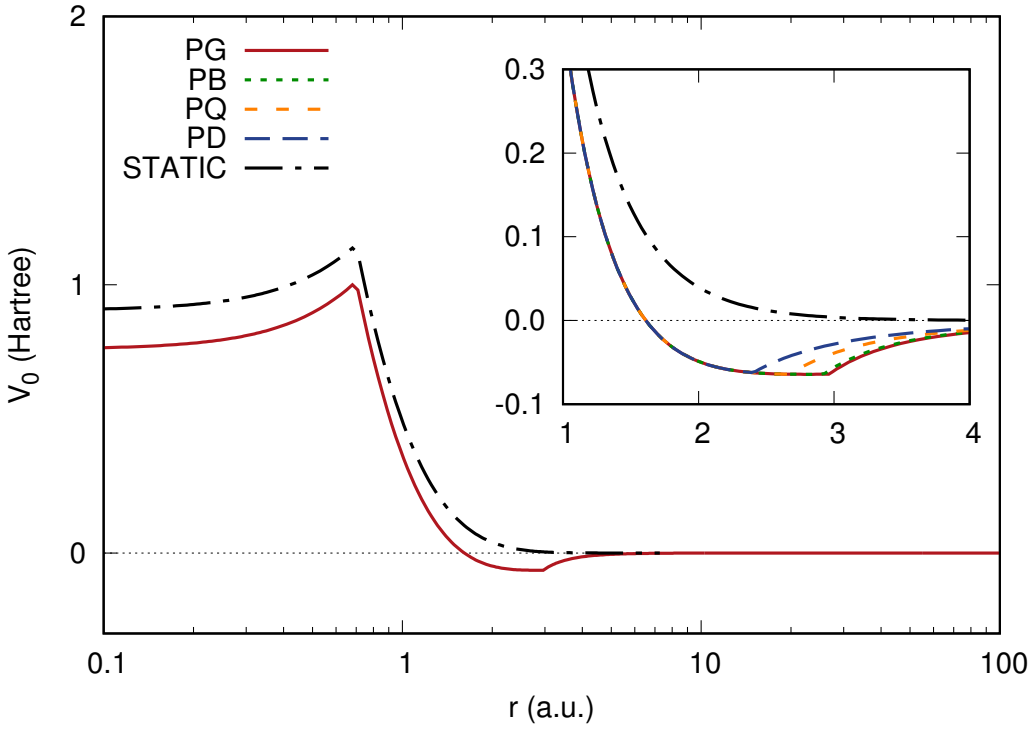

Figure 1. Spherical component of the positron-H_2 interaction potential with the abscissa and ordinate axis given in units of Borhs and Hartrees, respectively. The repulsive static potential is provided as the dashed-point black curve where we can readily identify the position of the H atom and the short range asymptotic behaviour of the potential. The static plus correlation-polarization potential is provided as the full curve where the reader can verify from the inset that the different levels of molecular polarization essentially affect the cut radius at the molecular border. Legends are the same as given in the text after Equation (7).

With the interaction potential fully defined, the scattering equation

$$|\psi\rangle = |u\rangle + G_0 V |\psi\rangle \tag{8}$$

can be solved. For this purpose we adopt the Method of Continued Fractions (MCF) as computationally implemented for electron scattering by Ribeiro et al. [48] and adapted for positron scattering by Tenfen [49,50]. This methodology has already been applied successfully in a series of contexts, including elastic electron scattering [48], electronic excitation by electron impact [51], photoionization [52] and positron scattering [38,45,53,54]. The theoretical details of the MCF have already been discussed elsewhere [48,49], so in this work we only discuss the numerical details for positron scattering by H_2.

3. Numerical Details

For the description of the molecular wave function of H_2, we adopted the Gaussian type orbitals as given in Table 2. The fixed nuclei Hartree-Fock calculation was performed at

the experimental equilibrium geometry $R_{H-H} = 1.401$ a.u. [55]. Within this approximation, we obtained the energy for the ground state level as $E_{SCF} = -1.133011$ Eh, the quadrupole moment $\Theta_{zz} = 0.4938$ a.u. and the hexadecapole moment $\Phi_{zz} = 0.2923$ a.u. All these values are consistent with the ones obtained in the same approximation with a much larger basis set by Maroulis and Bishop [56]. As stated previously, this level of agreement between the SCF properties with the literature values is an indication that our electron density is well described, and then it is expected that the correlation energy as given by Equation (6) is correct within the adopted approximation.

Table 2. Gaussian basis set adopted to describe the H_2 electron wave function. This basis is given by Dunning [57] with some augmenting functions.

Type	Exponents	Coefficients
s	33.6400	0.025374
	5.05800	0.189684
	1.14700	0.852933
s	0.32110	1.000000
s	0.10130	1.000000
s	0.04730	1.000000
p	1.12330	1.000000
p	0.27110	1.000000
p	0.06970	1.000000
d	0.53710	1.000000

The polarization potential given in Equation (7) is dependent on the polarizabilities of the molecule. In this study, we adopted the CISD/D6Z values determined by Miliordos and Hunt [58], and such values are given in Table 3. Since the polarizabilities enter in our calculations as parameters, we chose these values in order to satisfy the best long range polarization function possible. Also, it was a matter of convenience to select the tabulated data in [58] that was calculated at the equilibrium geometry. It seems that the α_Q value considered by Frighetto et al. [30] is in error by a factor of 2. Actually, Equation (7) is consistent with Dalgarno's definition [59], however the relation between Dalgarno and Buckingham quadrupole polarizabilities is $\alpha_q = 2C_0$ (see, for instance, Buckingham [60], Thakkar and Lupinetti [61] and Maroulis and Thakkar [62]). This is an important issue, and should be considered carefully when comparing their results and potential analysis.

Table 3. Polarizabilities obtained in the CISD/D6Z approach by Miliordos and Hunt [58].

Quantity	Value (a.u.)
α_0	5.1789
α_2	1.2103
α_Q	15.7793
B	−74.800
γ	620.27

All of our scattering calculations were carried out with the MCF, as stated previously, within a 800 radial grid points ranging from 0.002 to 125.35 a.u. Particular attention to the molecular region is given when distributing these radial points, and we found that 295 grid points up to 10.0 a.u. are enough to guarantee that the electronic wave function normalizes better than $1.0000 \pm 1 \times 10^{-4}$. Also, this grid is considered sufficient in terms of the electrostatic potential expansion as in Equation (3), since the obtained SCF quadrupole moment compares satisfactorily to the reference value.

Partial wave expansion was adopted to represent the scattering wave function, and generally $l_{max} = 6$ was adopted in such procedure. For energies lower than 1 eV, $l_{max} = 4$

was considered sufficient. However, it is well known that the small and large angle regions of the differential cross sections are strongly dependent on the l_{max} value, even when the integral cross section seems to be converged within the expansion. In order to compare the available experimental data with the best calculation possible, we extended the partial wave expansion up to $l_{max} = 14$ for the particular energies where experimental differential cross sections are available. With $l_{max} = 14$ the differential cross sections converged satisfactorily for energies up to 10 eV, leaving only the $\theta \to 0$ region to be corrected by a larger partial wave expansion or by a closure relation, as the O'Malley formula [63,64].

Folding the calculated differencial cross sections is necessary in order to compare with the experimental data of Sullivan et al. [65] and Machacek et al. [18], since their measured differential cross sections (DCS) are obtained as mirrored and summed around 90°. This is, even that we have access to the theoretical differential cross sections from 0 to 180° for every energy in the calculated range, we report only the folded differential cross sections $FDCS(\theta \leq 90°) = DCS(\theta) + DCS(180°-\theta)$ in order to directly compare our results to the experimental data.

Available total cross section (TCS) data is generally uncorrected for forward angle scattering [34]. This is the case for the TCS data from Zecca et al. [17], which we compare to our present results together with the measurements of Machacek et al. [18]. Both were corrected for the forward scattering effect with the theoretical data from Zammit et al. [29]. The measurements of Zecca et al. [17] are available for energies as low as 0.1 eV and our theoretical approach is fundamentally different from Zammit et al. [28], so we chose to employ the present calculated cross sections to correct this experimental data set. Since Zecca's cross section data goes for energies as low as 0.1 eV, the corrected cross sections may be valuable to analyze some properties of the positron H_2 system, such as the scattering length as done previously by Zhang et al. [36]. The conclusions of Zhang were criticized by Brunger et al. [34], so further discussion about these data may shed some light over this controversy.

To correct the measured total cross section data adopting the calculated cross sections one must know the critical missing angles for the spectrometer from where the data were measured, for each energy that there is a measurement. Transmission based spectrometers where the positron beam is guided by a magnetic field have a critical missing angle given by

$$\theta_c = \arcsin\left(\frac{eBr}{\sqrt{2mE}}\right), \tag{9}$$

where e is the positron charge, B is the magnitude of the guiding magnetic field, r is the gyration radius of the positron at the scattering cell exit, m is the positron mass and E is its kinetic energy. Since the critical missing angles were given for the Trento spectrometer by Zecca et al. [66], we took those values and interpolated with a function

$$\sin\theta_c = \frac{a}{\sqrt{E}}, \tag{10}$$

where a is some proportionality constant. Using the least squares regression method as implemented in gnuplot, we obtained $a = 0.300059$ eV$^{1/2}$. With this function, we selected the energy for which there is TCS measured data and determined the corresponding critical missing angle. These values are presented in Figure 2.

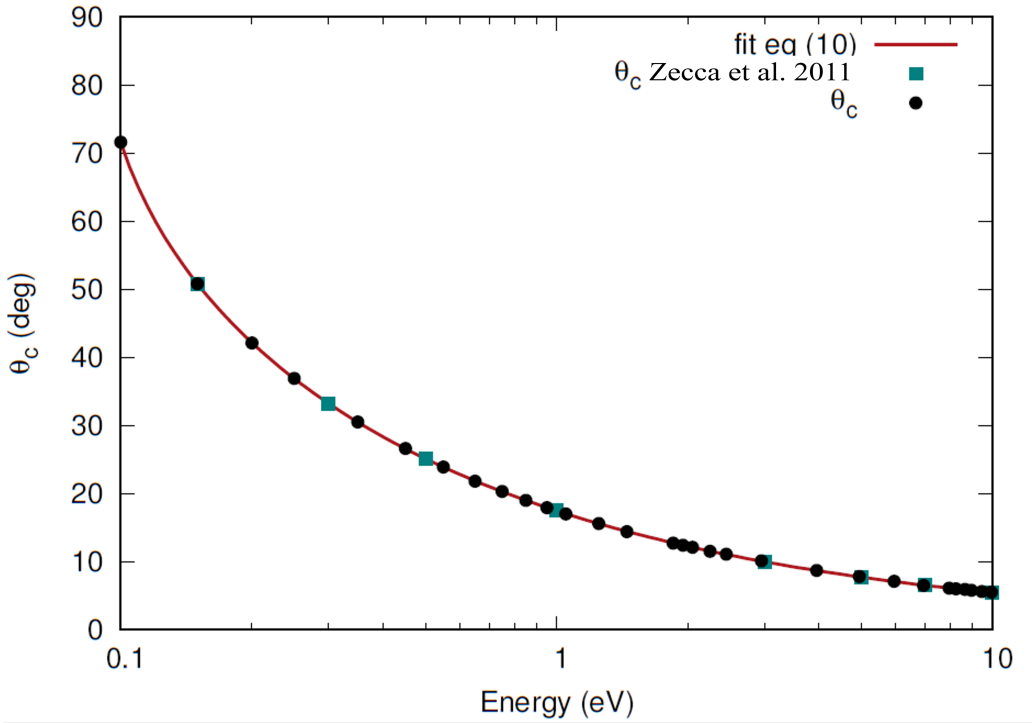

Figure 2. Original critical missing angles as given in Zecca et al. [66] (blue squares), the fitted function $\theta_c(E) = \arcsin\left(\frac{0.300059\,\mathrm{eV}^{1/2}}{\sqrt{E}}\right)$ (continuous red line) and the critical missing angles for each energy where there is a TCS measurement available in [17] (black filled circles).

Adopting the critical missing angles from reference [66] means that we are slightly overestimating the missing angles, since the guiding magnetic field was lower in [17]. Even so, the table given in [66] is the most complete data for the missing angle for the given spectrometer. We will compare the measurements with our theoretical results and correct the experimental TCS even with a little overestimation on the critical angle. Once the critical missing angle is known for a given energy, the correction of the measured cross section is very straightforward. Following Brunger et al. [34] and Sullivan et al. [33], we define the corrected TCS as

$$\sigma_c = \sigma_m + 2\pi \int_0^{\theta_c} \frac{d\sigma_{teo}}{d\Omega} \sin\theta d\theta, \tag{11}$$

where σ_m is the forward uncorrected measured TCS and $\frac{d\sigma_{teo}}{d\Omega}$ is the theoretical differential cross section for the corresponding energy. Since we resolve our calculated cross sections angle by angle, a simple trapezoid rule is adopted to solve the numerical integration. We also integrate the calculated differential cross section and compare it to the integral cross section given by the optical theorem, to guarantee that our integration procedure is appropriate for every angular range and energy considered.

4. Results and Discussion

4.1. Phase Shifts and ICS

We determined the scattering phase shifts within the different described approaches, and present the calculated values for $l = 0$ in Figure 3 and for $l = 1$ in Figure 4. For direct comparison, we have elected the most recent phase shifts from Rawlins et al. [13] and from Frighetto et al. [30].

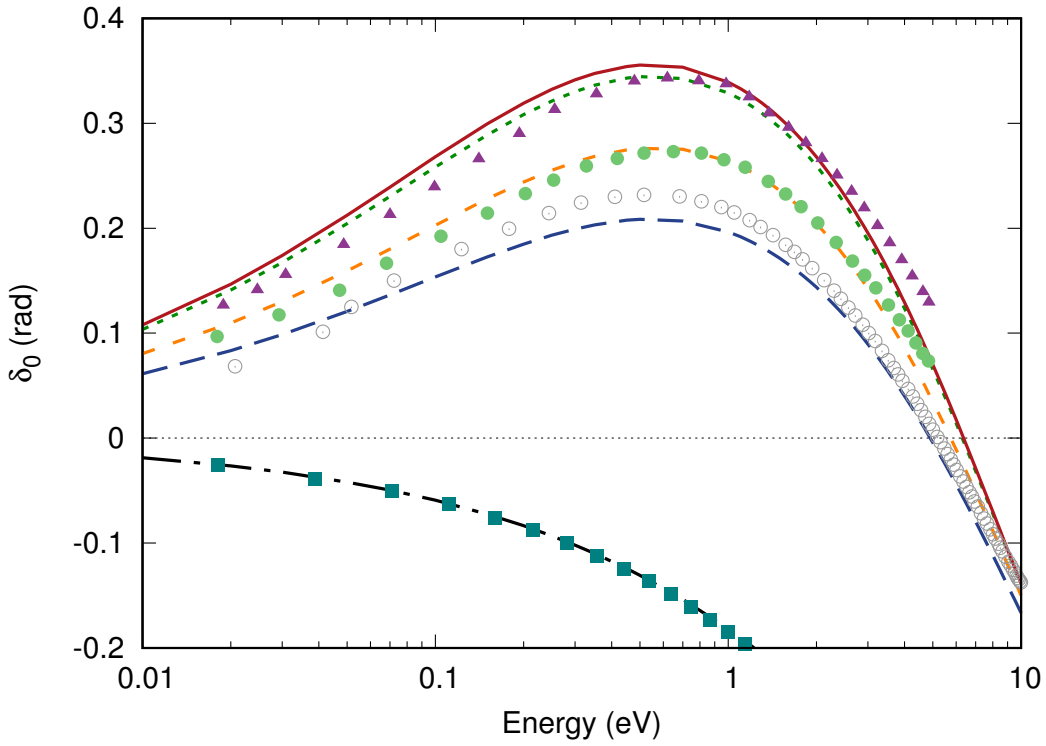

Figure 3. *s*-wave phase shifts obtained in the present work adopting the different polarization approaches as discussed around Equation (7) compared to the values from Rawlins et al. [13] and Frighetto et al. [30]. Present results: black dash dotted line represents the δ_0 obtained within the electrostatic approximation, while PD is given by the blue long dashed line, PQ is the yellow short dashed line, PB is the dotted green line and PG is the red solid line. The blue squares represent the results in the static approximation, the purple triangles are the GW + Γ results and the light green circles are the GW + Γ + Λ results from Rawlins et al. [13]. The grey open circles is the SMC-SP results from Frighetto et al. [30].

First of all, we compare our static *s*-wave phase shifts, given by the black dash dotted line, with the equivalent HF results from Rawlins et al. [13], presented in blue solid squares. Even that our basis set is much more simple than that adopted by Rawlins et al. [13], our static phase shifts compare very well, which means that our representation of the electrostatic effects over the scattering process is nearly identical. Our present correlation polarization approaches are represented in Figure 3 by the blue long dashed line (PD), the yellow short dashed line (PQ), the green dotted line (PB) and the red solid line (PG). The accurate many body results from Rawlins et al. [13] are given by the solid magenta triangles (GW + Γ) and the solid light green circles (GW + Γ + Λ). We chose to compare only these two approaches to our results since they are the only that include virtual positronium formation. We can see that the approaches PB and PG compare satisfactorily with the overcorrelated GW + Γ approach from reference [13]. The PQ approach compares very well with the GW + Γ + Λ results from Rawlins et al. [13], which can be considered the best many body approach from that work. This suggests that our incomplete perturbative series given by the PQ approach should be considered the approach that better describe the positron molecule interaction in the present work. This conclusion, combined with the fact that the polarization interaction only converges at the PG level, have two important meanings: (1) the correlation potential given by Equation (6) does not represent correctly the correlation for the H_2 molecule; (2) even though the correlation is unbalanced from the polarization at r_{cut}, the correlation expression given by Equation (6) includes satisfactorily the virtual positronium formation in the form of a potential, given that r_{cut} is sufficiently close to the van der Waals radius of the molecule. The other approaches from reference [13]

that do not include the virtual positronium formation are systematically below our PD results, reinforcing the idea that some of the virtual positronium formation may be included even in the PD approach due to the magnitude of the correlation potential. Also, the recent results from Frighetto et al. [13], represented by the grey open circles, compare very well with our PD approach as we observed in our previous study on positron scattering by F_2 [45], which indicates that their methodology is unable to account for the full polarization interaction. It should be noted that it was recently demonstrated by Seidel and Arretche [67] that the SMC functional does not include the virtual positronium formation, which justify its inability to fully include the polarization effects even in the recent formulation of that methodology. Given the quality of the results obtained by Rawlins et al. [13] and the satisfactory comparison of our PQ results to their data, we will consider that for positron H_2 scattering the PQ approach is more realistical until the correlation energy can be fixed somehow (multiplication by a scaling factor or the justification of the r_{cut} value based on physical reasoning [44]).

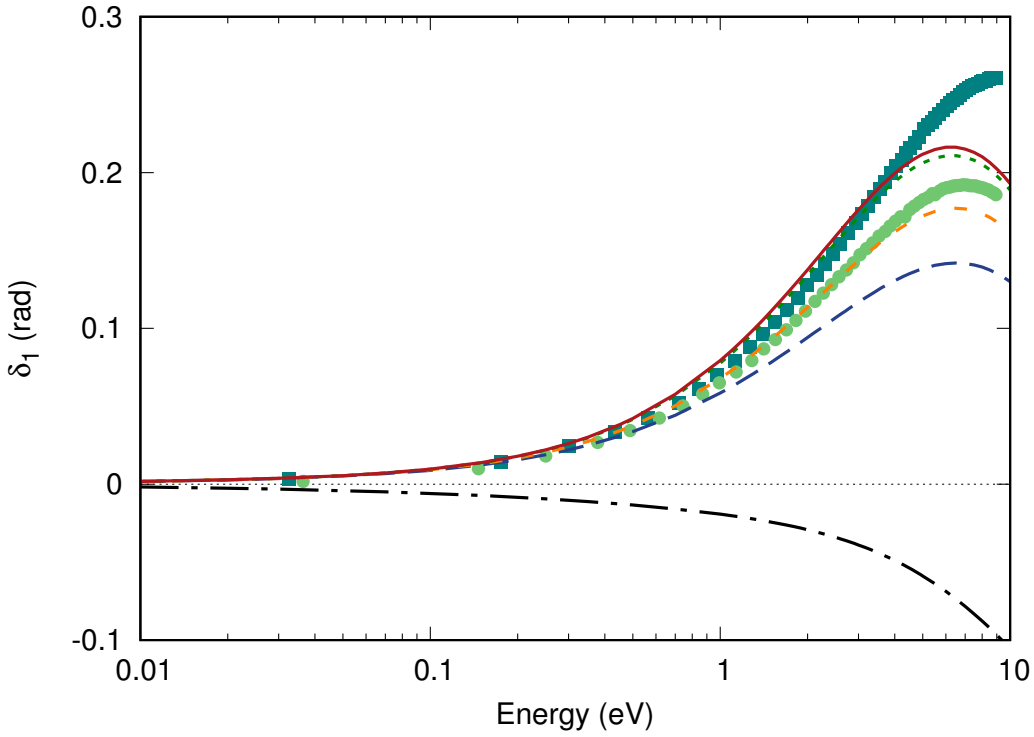

Figure 4. *p*-wave phase shifts obtained in the present work adopting the different polarization approaches as discussed around Equation (7) compared to the MERT fits from Fedus et al. [68]. The present results for each polarization approximation is given by the same curve and color as in Figure 3. The blue squares represent the MERT fitted data from the forward uncorrected measurements and the light green circles represent the fitted data from the forward corrected measurements of Machacek et al. [18].

In Figure 4 we compare our *p*-wave phase shifts to the MERT fits of Fedus et al. [68]. Our correlation polarization approaches are described by the same curves and colors as in Figure 3. The two MERT fits of Fedus et al. [68] are from the forward corrected and uncorrected TCS data of Machacek et al. [18]. The *p*-wave phase shifts from the forward corrected data is represented by the solid light green circles, and the fits from the uncorrected data is represented by the blue solid squares. It is noticeable that the forward scattering effects are not affected by the *p*-wave up to around 1 eV, where the MERT phase shifts from the corrected and uncorrected data begin to diverge. Our PB and PG *p*-wave phase shifts agree very well with the MERT fitted phase shifts for the forward uncorrected TCS data up

to 4 eV. Our PQ model, considered to represent correctly the scattering dynamics for the *s*-wave, agrees very well with the MERT *p*-wave phase shifts from the forward corrected data. The PD model, as expected, underestimates the polarization interaction since it is based on an unconverged perturbation series, diverging from the MERT data for energies below 1 eV. For energies around 4 eV, the *p*-wave is already dominant in the calculated ICS, so the fact that the *p*-wave phase shifts are below the MERT fitted values indicates that the PQ ICS will be below the measured TCS, corrected or uncorrected for forward scattering effects. To solve this discrepancy it is necessary to include the anisotropic terms for the quadrupole polarizability, the mixed first hyperpolarizability and the second dipole hyperpolarizability. All of these values are given by the respective tensors [41,62], and the inclusion of such polarization interaction in the scattering model potential is expected to enhance the calculated integral cross sections for energies larger than 4 eV. It is also noticeable from Figure 3 that our PQ results diverge substantially from the GW + $\Gamma + \Lambda$ for energies around 4 eV, which also indicates that the coupling between the $l = 2$ term of the potential and the *s* and *p* terms of the scattering wave function is considerable in this energy range. Complementing this figure we present our electrostatic *p*-wave phase shifts, given as a black dash dotted line as in Figure 3. We notice that while this phase shifts curve have the correct trend, there is no corresponding data in the literature to compare with.

All of the aspects observed in the phase shift curves are expected to manifest in the ICS curves, which we present in Figure 5. Once again all of our approaches are represented by the same curves and colors scheme, and we included the ICS reported by Rawlins et al. [13] as the light green dash dotted curve. Even that there are other many body ab initio results in the literature [28–30], we chose to compare with just the theoretical results which include explicitly the virtual positronium effects and also present the *s*-wave phase shifts, which is very helpful in the interpretation of the results. For the experimental TCS we present the forward corrected measurements of Machacek et al. [18] as the solid magenta triangles, the uncorrected and unscaled [34] data of Zecca et al. [17] as the open black circles and the measurements of Zecca et al. [17] corrected for the forward scattering effects with our PQ differential cross sections as the solid black circles. It can be seen from the comparison that the ICS reported by Rawlins et al. [13] is systematically above our PQ curve, which reinforces the idea that the *p*-wave is underestimated in all of our approaches. Still, the agreement between our PQ ICS and the results reported by Rawlins et al. [13] is rather good up to around 4 eV, where the *p*-wave effects become more significant. The magnitude of the ICS obtained in the PB and PG approaches is clearly overestimated according to the available experimental data, and there is no expectation that any measured cross section data will follow these curves. Finally, the ICS obtained from the PD model is below every other presented result due to lack of long range polarization effects, particularly at the peripheral region of the molecule. The agreement of this curve to the forward corrected data from Zecca et al. [17] (black solid circles) is artificial, since the forward effects were considered through the PQ differential cross sections, which are substantially larger than the PD ones at forward scattering angles.

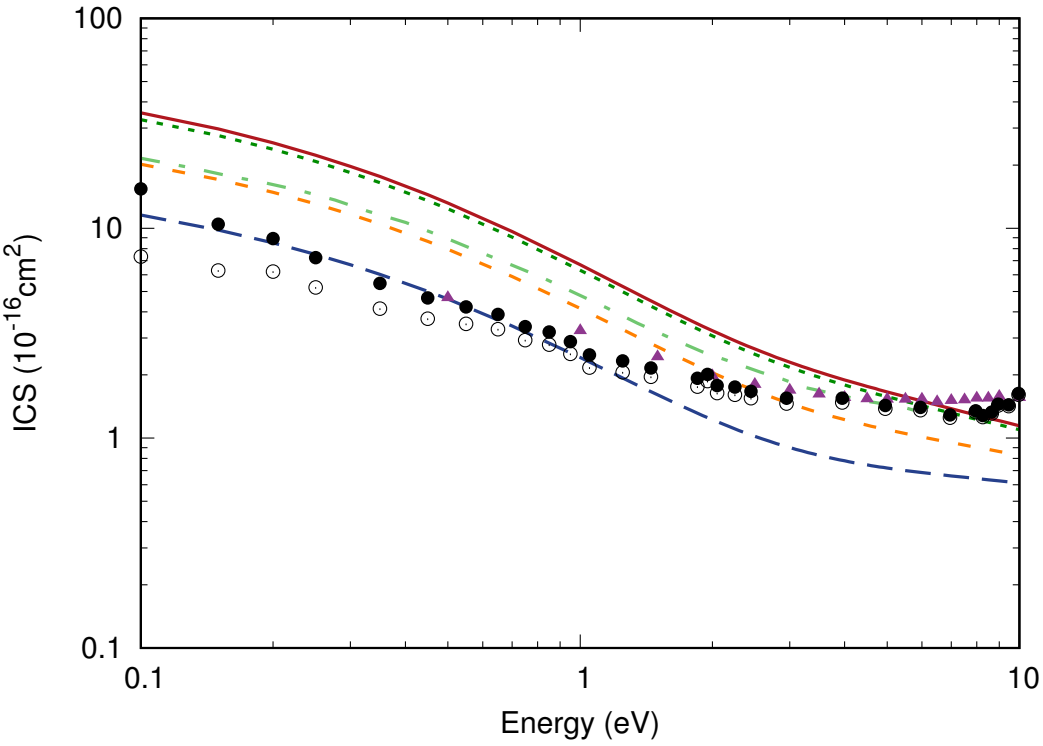

Figure 5. Present ICS compared to the theoretical results of Rawlins et al. [13] (light green short dashed dotted line) and to the experimental data of Machacek et al. [18] (magenta triangles) and Zecca et al. [17] (open black circles—original data, filled black circles—forward corrected data). The present results for each polarization approximation is given by the same curve and color as in Figure 3.

4.2. DCS and Forward Scattering Effects

The only set of measured differential cross sections is from Sullivan et al. [65] and Machacek et al. [18], where they adopted a methodology capable of obtaining the differential cross sections from a transmission based technique. While this is a very interesting method, capable of providing crucial information about the polarization in positron scattering by molecules [69], it has the drawback of being folded, this is, the DCS for each angle θ up to 90° is summed to the DCS value of 180°$-\theta$, mixing the information of the low angle region, which responds strongly to the polarization effects, to the high scattering angle region, dependent on the repulsive electrostatic interaction. Although it seems to be possible to unfold such differential cross sections through a partial wave fitting procedure [70], the low energy differential cross sections would still be affected by the forward scattering effects [34], unavoidable in transmission based experiments, and rescattering [71]. As we can see in Figure 5, the forward scattering effect corrections are expected to be significant up to around 3 eV.

We begin to discuss the FDCS where the forward scattering corrections are expected to be significant, as illustrated in Figure 5. Figure 6 presents the FDCS measurements of Sullivan et al. [65] in panel (a) for 0.5 eV and Machacek et al. [18] in panel (b) for 1.0 eV, both compared to the polarization approximations discussed in this work and the MERT data of Fedus et al. [68]. For 0.5 eV, we note that the experimental data agrees qualitatively and in magnitude with the PD approximation and the MERT data extracted from the TCS measurements without forward scattering corrections [68], up to around 50°. For higher angles, the measured FDCS seems to follow a different trend, which seems to be due to rescattering effects as described by [71]. This partial agreement can be justified by the comparison of the present PD data with the corrected and uncorrected TCS of Zecca et al. [17], as we can observe in Figure 5. Even that the experimental approaches for

the obtention of the TCS and FDCS are different, both give absolute values, thus some level of quantitative aggrement observed on the TCS data should also be observed on the FDCS. Since for this energy the forward scattering effects are expected to play a significant role in the scattering dynamics, we suggest that a DCS measurement from a crossed beam experiment, or the FDCS once corrected for forward scattering and rescattering effects, to compare qualitatively and quantitatively with the PQ curve or to be between PQ and the forward corrected MERT data. In order to provide such comparison, we propose that the FDCS should be corrected for the forward scattering effects uniformily, this is, the FDCS measured for each angle should be added to a correction factor Δ so the integrated FDCS corresponds to the forward corrected TCS as

$$\sigma_c = 2\pi \int_0^{\pi/2} (FDCS + \Delta) \sin\theta d\theta \tag{12}$$

where σ_c has the same meaning as in Equation (11). For this particular energy, we corrected the TCS of Machacek et al. [18], adopting their θ_c tabulated values and extrapolating those values as a function of $1/\sqrt{E}$. The forward scattering effect correction factor σ_{corr} ($\sigma_c = \sigma_m + \sigma_{corr}$) for this energy was determined, and then equating it to the correction over the integrated FDCS we obtained

$$\Delta = \frac{\sigma_{corr}}{2\pi}. \tag{13}$$

Adopting the PQ DCS at 0.5 eV to correct the TCS of Machacek et al [18], as we did for the TCS measurements of Zecca et al. [17], the obtained value for this correction factor is $\Delta \approx 0.21$ Å^2/sr. The FDCS summed to this correction factor is presented in panel (a) of figure 6 as the black open circles. As we antecipated, the values are between the PQ and the forward corrected MERT of Fedus et al. [68]. Still, the rescattering effects are unaccounted for.

The FDCS correction factor value obtained above is reinforced by the comparison between the corrected and uncorrected data of Zecca et al. [17] as seen in Figure 5, as the correction represents 25.6% at 0.45 eV and 20.5% at 0.55 eV, so the correction should be around 23% at 0.5 eV. While the angular resolution of Trento and ANU spectrometers are different, we can evaluate this correction to the measured FDCS from them as a rough estimate. With this assumption, we obtain $\Delta \approx 0.17$ Å^2/sr, which is sufficiently close to the value obtained by explicitly correcting the measured TCS for the forward scattering effects. It must be noted that the TCS measurements of Zecca et al. [17] seems to be undervaluated at the low energy range, as noted by Zhang et al. [36] based on the scattering length value. Also, the recommended data of Brunger et al. [34] for this energy is Zecca's original data multiplied by a scale factor of 1.2954. Also, Pinheiro et al. [72] indicated that the very low energy data of the Trento spectrometer may have other problems than just the forward scattering. Anyway, we expect that the corrected and uncorrected TCS data from Figure 5 to be somewhat larger, also getting closer to the PQ curve magnitude. A revisit on very low energy positron scattering by H_2 is necessary in order to address these questions.

For 1.0 eV, as given in panel (b) of Figure 6, we note a better agreement between the experimental FDCS of Machacek et at. [18] and the PQ curve. As for 0.5 eV, we notice that the measured FDCS presents two different qualitative trends: from 20° to 50° the FDCS seems to follow the qualitative behaviour of every curve presented in panel b), while for angles larger than 50° a linear decay can be observed. Once again, this effect appears to be due to rescattering as discussed for positron scattering from Ne by Cheong et al. [71]. From Figure 5, we note that the corrected and uncorrected data of Zecca et al. [17] are slightly below the corrected data of Machacek et al. [18], while the 1.0 eV TCS as measured by the

ANU group is almost in the same magnitude of the PQ ICS. This means that the forward scattering effects for this energy are much less significant than for lower energies. The agreement between the 1.0 eV measured FDCS and the PQ approach is an indication that the forward scattering effects are getting smaller. The structures present in the measured FDCS at around 30° and 50° are not observed in any other theoretical approach, which generally do not consider vibrational and rotational target excitations.

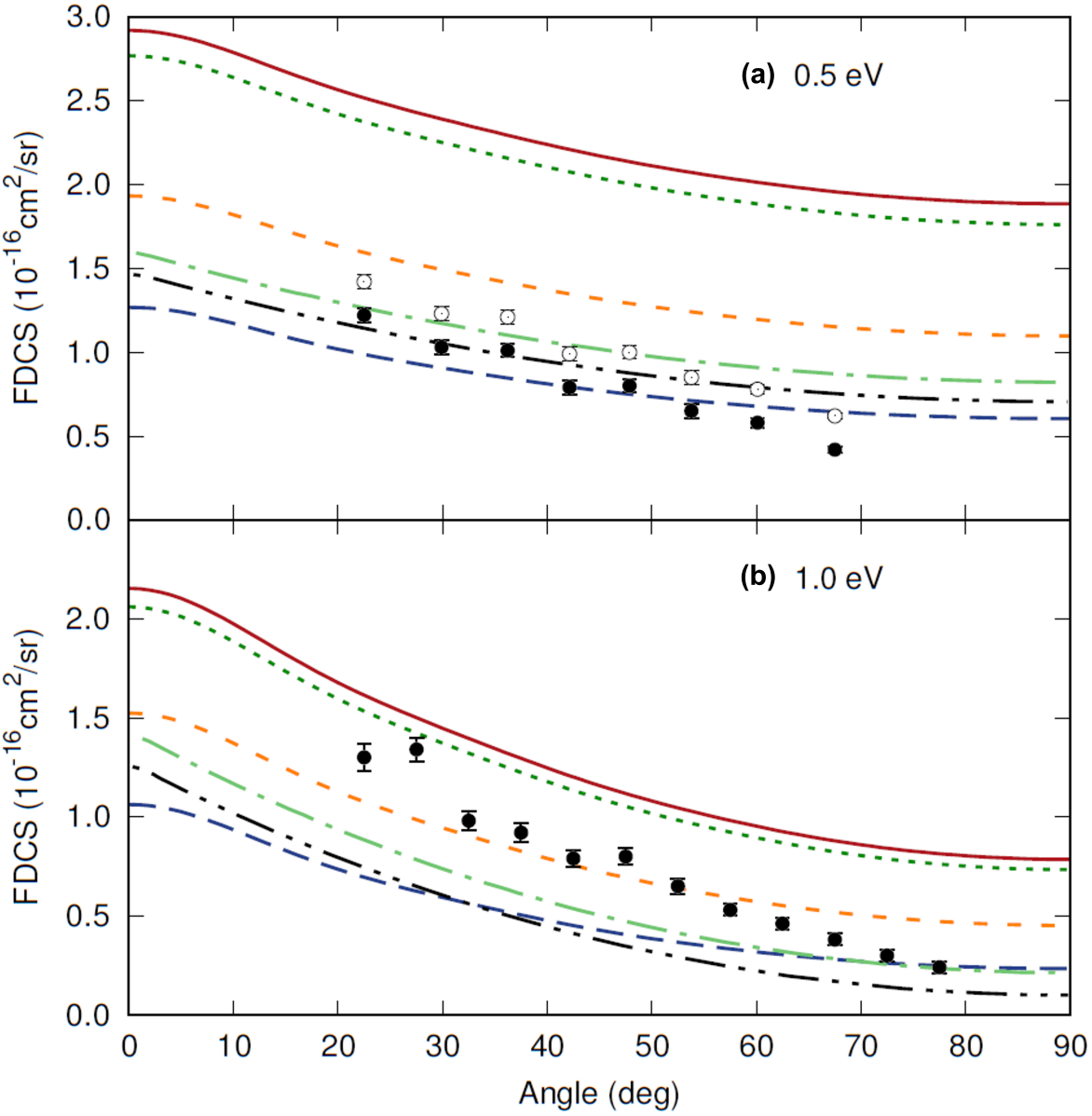

Figure 6. Present FDCS for 0.5 eV in panel (**a**) and 1.0 eV in panel (**b**) compared to the experimental data of Sullivan et al. [65] panel (**a**) and Machacek et al. [18] panel (**b**), and the MERT derived FDCS from Fedus et al. [68]. In panel (**a**) we present also the measured FDCS of Sullivan et al. [65] corrected for the forward scattering effects as the open black circles (see details in the text). The MERT data of Fedus et al. [68] is presented as the long dash dotted light green line (forward corrected) and the long dashed double dotted black line (forward uncorrected). The present results for each polarization approximation is given by the same curve and color as in Figure 3.

As we can see in Figure 5, the forward scattering corrections are significant only up to 3.0 eV. This is, the FDCS presented in Figure 7 supposedely are not strongly influenced by low angle scattering. At this energy, the FDCS measured by Machacek et al. [18] compare satisfactorily with PB and PG models for folded angles lower than 30°. For larger angles,

the FDCS is in better agreement to the PQ model and the corrected and uncorrected MERT data from Fedus et al. [68]. A closer inspection of the ICS given in Figure 5, reveals that for this energy the calculated ICS in any model presented in this work is deficient in anisotropic polarization effects. This idea is reinforced by the comparison of *p*-wave phaseshifts given in Figure 4, where the PQ phaseshift begin to diverge significantly from the corrected MERT one, which in principle contains such effects. The comparison between the FDCS and the curves obtained from the models presented in this work, indicates that the anisotropic polarization effects may influence the DCS at the low angle region, i.e., for angles lower than around 30° or 40°. Once these polarizations are included in the scattering model, it is expected that the PQ curve becomes more forward peaked, comparing satisfactorily to the measured FDCS.

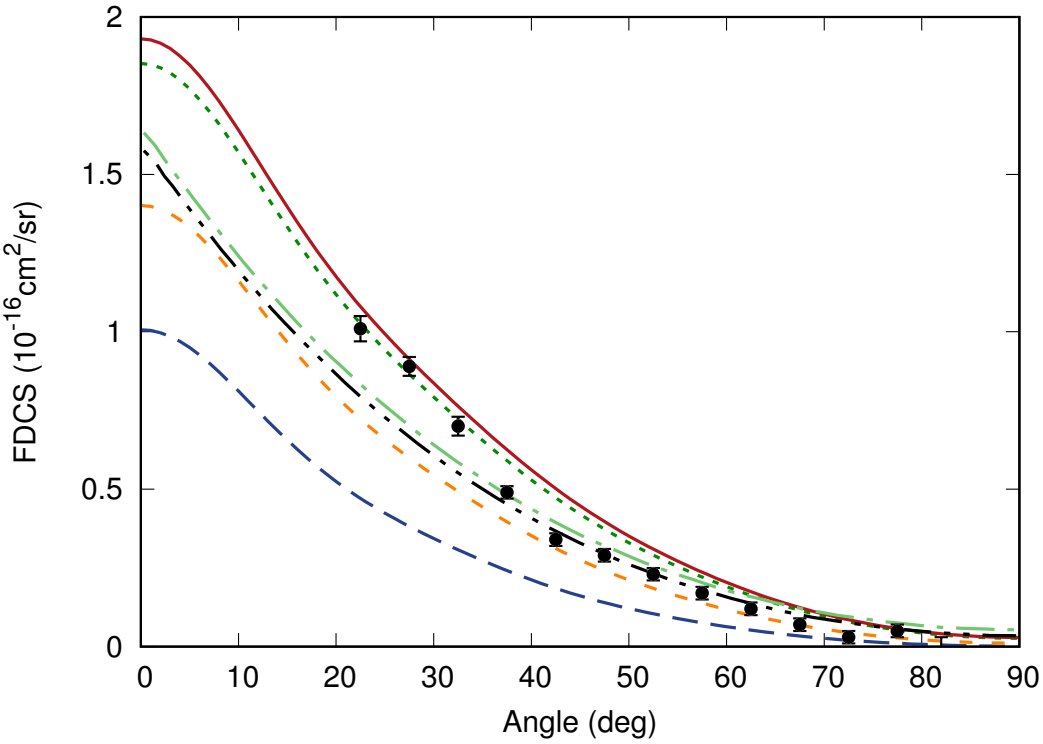

Figure 7. Present FDCS for 3.0 eV compared to the experimental data of Machacek et al. [18] and the MERT derived FDCS from Fedus et al. [68]. The MERT data of Fedus et al. [68] is presented as the long dash dotted light green line (forward corrected) and the long dashed double dotted black line (forward uncorrected). The present results for each polarization approximation is given by the same curve and color as in Figure 3.

Finally we present in Figure 8 the FDCS obtained in the present work compared to the measurements of Machacek et al. [18] for 7.0 eV in panel (a) and 10.0 eV in panel (b). As Figure 5 indicates, the forward scattering corrections for the TCS at these energies are insignificant, and so it is expected to be for the experimental FDCS. Once again, the deficiency in the description of the anisotropic polarization effects in the present scattering model is manifest in the presented PD, PQ, PB and PG curves. The MERT data naturally contains such effects, for being determined from a fit procedure to the experimental TCS. As for 3 eV, we expect that the inclusion of these effects in the scattering model will enhance the comparison between the model approaches to the experimental data in the lower angle region. For 10 eV (panel b) we can also notice the presence of a shallow minimum in the measured FDCS and in the model calculations, however the MERT data is monotonic. It is unclear why the MERT data does not follow the qualitative trend of the measured FDCS, however the presence of such minimum in the present models is an indication

that the correlation and polarization scheme adopted in this work can describe correctly the scattering dynamics, even that some adjustments to the magnitude of the correlation component at the van der Waals radius are still necessary.

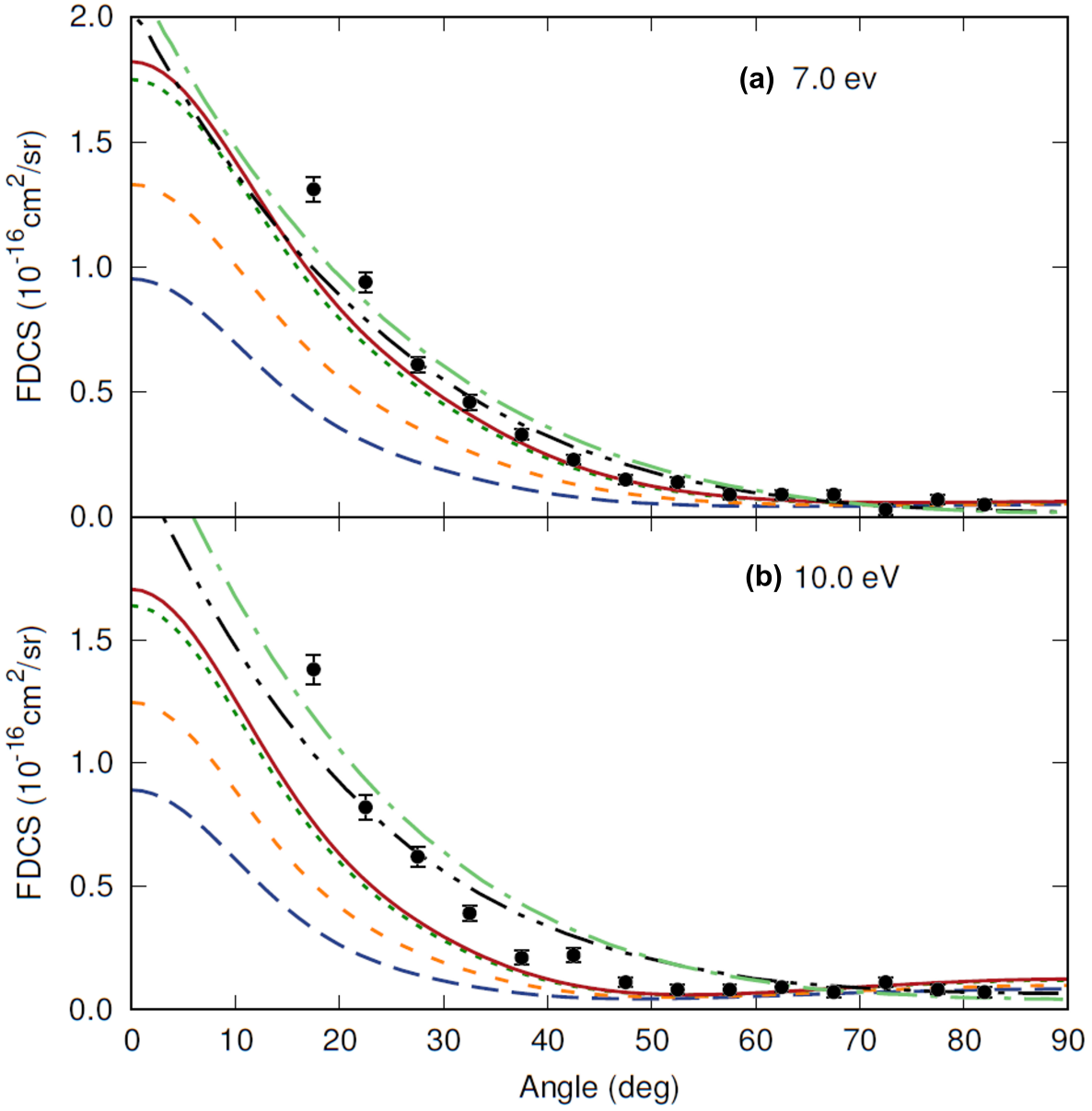

Figure 8. Present FDCS for 7.0 eV in panel (**a**) and 10.0 eV in panel (**b**) compared to the experimental data of Machacek et al. [18] and the MERT derived FDCS from Fedus et al. [68]. The MERT data of Fedus et al. [68] is presented as the long dash dotted light green line (forward corrected) and the long dashed double dotted black line (forward uncorrected). The present results for each polarization approximation is given by the same curve and color as in Figure 3.

4.3. Scattering Length and Possible Corrections to the Model

It is well known that the scattering length is a fundamental quantity for the characterization of the low energy scattering. This value has been reported for positron scattering by H_2 by Zhang [36], Rawlins et al. [13] and Zammit et al. [29] from the theoretical side, while Fedus et al. [68] report the MERT scattering lenght from experimental data of Machacek et al. [18], Karwasz et al. [73] and Zecca et al. [17]. In Table 4 we present the scattering length for each polarization model adopted in this work and the other values available in the literature. The comparison between the values from this work to the previous calculations and experimental estimatives, shows that the A_0 value obtained

from the PQ approach, $A_0 = -3.124$ a.u., is somewhat overestimated, as expected from the previous discussions. It is 15% larger than the value $A_0 = -2.73$ a.u. obtained by Rawlins et al. [13]. On the other hand, the PD approach gives a scattering length that is only 12% below the value obtained by Rawlins et al. [13]. While this seems to qualify the PD or the PQ approaches, the converged polarization interaction is given by the PG one. A comparison between the values presented in Tables 1 and 4 shows that the scattering length is strongly dependent on the r_{cut} value, so an indication on how to fix the correlation potential is to multiply it by a factor that results in a scattering length obtained with full polarization that is sufficiently close to -2.73 a.u. The way this new r_{cut} compares with the van der Waals radius may serve as a criterium to fix the correlation interaction for targets which we do not have information about the scattering length or any kind of experimental data. This is a matter to be investigated in further works.

Table 4. Values for the scattering length obtained in the different polarization approximations. All values were determined for $E = 1 \times 10^{-6}$ eV.

Model	A_0 (a.u.)
PD	-2.390
PQ	-3.124
PB	-4.015
PG	-4.178
Zhang [36]	-2.63
Zammit [29]	-2.72
Rawlins [13]	-2.73
Machacek [18]	-2.67 ± 0.02
Karwasz [73]	-2.71 ± 0.02
Zecca [17]	-2.09 ± 0.02

5. Conclusions

In this work we investigated the scattering of low energy positrons by H_2 molecules adopting a polarization correlation model (PCOP) and explored the effects of second, third and fourth order perturbation theory polarization. An inspection of the scattering potential shows that the polarization up to fourth order is necessary in order to achieve convergence, however the calculated cross sections are larger than the most recent many body ab initio calculation that explicitly includes the effects of virtual positronium. The agreement of the present PQ model to the results presented by Rawlins et al. [13], suggests that the overcorrelation introduced by the PCOP functional in the vicinity of the van der Waals radius can model efficiently the effects of virtual positronium formation.

Special attention was given to the correction for the forward scattering effects over the TCS measurements of Zecca et al. [17] and to the comparison of the obtained results with the FDCS measurements of Sullivan et al. [65] and Machacek et al. [18]. Since the FDCS measuring method is affected by the angular resolution of the spectrometer, we proposed a correction to the magnitude of the experimental FDCS at 0.5 eV, based on the direct correction of the TCS data of Machacek et al. [18] for forward scattering effects and also from the estimated correction for these over Zecca's TCS. In spite of the correction methodology being simple, the corrected FDCS presents quantitative agreement to the PQ model and also to the MERT [68] one extracted from forward corrected data of Machacek et al. [18], which gives some level of confidence that the correction is necessary and the adopted method is reliable. For other energies, the comparison of the present results to the measured FDCS from Machacek et al. [18] suggests that the inclusion of anisotropic terms from the polarization interaction are necessary in order to the calculated ICS and DCS to reach the correct magnitude.

The calculated scattering length for each of the polarization models explored in this work, and their comparison to other values from the literature, indicates that the PD model is undercorrelated while the PQ, PB and PG models are overcorrelated. Since all other terms in the scattering potential are exact to within reasonable numerical accuracy, this means that adjustments over the magnitude of the correlation term at the molecular border may be necessary in order to the adopted potentials to correctly describe the available scattering observables. These adjustments to the correlation potential will qualify the approach as semi empirical as in reference [74], which is adequate to identify characteristics of the scattering potential necessary in a self sufficient methodology. Further works will be developed to this end.

Author Contributions: Conceptualization, W.T., J.d.S.G., S.E.d.S.S., E.P.S. and F.A.; methodology, W.T., J.d.S.G., S.E.d.S.S., E.P.S. and F.A.; formal analysis, W.T., J.d.S.G., S.E.d.S.S., E.P.S. and F.A.; writing, W.T., J.d.S.G., S.E.d.S.S., E.P.S. and F.A. All authors have read and agreed to the published version of the manuscript.

Funding: The financial support for this study from Gdansk University of Technology, Poland by the DEC-45/2023/IDUB/I.

Data Availability Statement: The raw data supporting the conclusions of this article will be made available by the authors on request.

Acknowledgments: F. Arretche acknowledge the support from Conselho Nacional de Desenvolvimento Científico e Tecnológico (CNPq), Brazil. Financial support of this study from Gdańsk University of Technology, Poland by the DEC-45/2023/IDUB/I.1. grant under the NOBELIUM Joining Gdańsk-Tech Research program (E.P. Seidel) is gratefully acknowledged. J.d.S. Glória and S.E.d.S. Saab acknowledge Coordenação de Aperfeiçoamento de Pessoal de Nível Superior (CAPES), Brazil, Finance Code 001, for the MSc Scholarships. Also, the authors would like to thank the Programa de Pós-Graduação em Física of Universidade Federal de Santa Catarina and Universidade Federal de Pelotas for the support.

Conflicts of Interest: The authors declare no conflict of interest.

Abbreviations

The following abbreviations are used in this manuscript:

TCS	Total Cross Sections
PCOP	Positron Correlation Polarization
SCP	Static Correlation Polarization
HF	Hartree-Fock
PD	Dipolar Polarization
PQ	Quadrupolar Polarization
PB	First Hyperpolar Polarization
PG	Second Hyperpolar Polarization
MCF	Method of Continued Fractions
SCF	Self Consistent Field
CISD	Configuration Interaction Singles and Doubles
DCS	Differential Cross Section
FDCS	Folded Differential Cross Section
MERT	Modified Effective Range Theory
ICS	Integral Cross Section

References

1. Helm, R.; Lehtonen, J.; Mayerhofer, M.; Mitteneder, J.; Egger, W.; Verbeke, R.; Sperr, P.; Dollinger, G.; Dickmann, M. Positron-annihilation lifetime spectroscopy with in-situ control of temperature, pressure and atmosphere to determine the free-volume of soft materials. *Nucl. Instruments Methods Phys. Res. Sect. Beam Interact. Mater. Atoms* **2024**, *549*, 165263. [CrossRef]
2. Shokoya, M.M.; Benkő, B.M.; Süvegh, K.; Zelkó, R.; Sebe, I. Positron annihilation lifetime spectroscopy as a special technique for the solid-state characterization of pharmaceutical excipients, drug delivery systems, and medical devices—A systematic review. *Pharmaceuticals* **2023**, *16*, 252. [CrossRef]
3. Charlton, M.; Giles, T.; Lewis, H.; Van Der Werf, D.P. Positron annihilation in small molecules. *J. Phys. B At. Mol. Opt. Phys.* **2013**, *46*, 195001. [CrossRef]
4. Blanco, F.; Muñoz, A.; Almeida, D.; Ferreira Da Silva, F.; Limão-Vieira, P.; Fuss, M.C.; Sanz, A.G.; García, G. Modelling low energy electron and positron tracks in biologically relevant media. *Eur. Phys. J. D* **2013**, *67*, 199. [CrossRef]
5. Hioki, T.; Gholami, Y.H.; McKelvey, K.J.; Aslani, A.; Marquis, H.; Eslick, E.M.; Willowson, K.P.; Howell, V.M.; Bailey, D.L. Overlooked potential of positrons in cancer therapy. *Sci. Rep.* **2021**, *11*, 2475. [CrossRef] [PubMed]
6. Le Loirec, C.; Champion, C. Track structure simulation for positron emitters of medical interest. Part I: The case of the allowed decay isotopes. *Nucl. Instruments Methods Phys. Res. Sect. A Accel. Spectrometers, Detect. Assoc. Equip.* **2007**, *582*, 644–653. [CrossRef]
7. Guessoum, N.; Jean, P.; Gillard, W. The lives and deaths of positrons in the interstellar medium. *Astron. Astrophys.* **2005**, *436*, 171–185. [CrossRef]
8. Guessoum, N.; Jean, P.; Gillard, W. Relevance of slow positron beam research to astrophysical studies of positron interactions and annihilation in the interstellar medium. *Appl. Surf. Sci.* **2006**, *252*, 3352–3361. [CrossRef]
9. Guessoum, N.; Jean, P.; Gillard, W. Positron annihilation on polycyclic aromatic hydrocarbon molecules in the interstellar medium. *Mon. Not. R. Astron. Soc.* **2010**, *402*, 1171–1178. [CrossRef]
10. Guessoum, N. Positron astrophysics and areas of relation to low-energy positron physics. *Eur. Phys. J. D* **2014**, *68*, 137. [CrossRef]
11. Mitroy, J.; Ivanov, I.A. Semiempirical model of positron scattering and annihilation. *Phys. Rev. A* **2002**, *65*, 042705. [CrossRef]
12. Gribakin, G.F.; Ludlow, J. Many-body theory of positron-atom interactions. *Phys. Rev. A* **2004**, *70*, 032720. [CrossRef]
13. Rawlins, C.; Hofierka, J.; Cunningham, B.; Patterson, C.; Green, D. Many-body theory calculations of positron scattering and annihilation in H_2, N_2, and CH_4. *Phys. Rev. Lett.* **2023**, *130*, 263001. [CrossRef]
14. Coleman, P.G.; Griffith, T.C.; Heyland, G.R. Measurement of total scattering cross-sections for positrons of energies 2–400 eV on molecular gases: H_2, D_2, N_2, CO. *Appl. Phys.* **1974**, *4*, 89–90. [CrossRef]
15. Charlton, M.; Griffith, T.C.; Heyland, G.R.; Wright, G.L. Total scattering cross sections for intermediate-energy positrons in the molecular gases H_2, O_2, N_2, CO_2 and CH_4. *J. Phys. B At. Mol. Phys.* **1980**, *13*, L353–L356. [CrossRef]
16. Hoffman, K.R.; Dababneh, M.S.; Hsieh, Y.F.; Kauppila, W.E.; Pol, V.; Smart, J.H.; Stein, T.S. Total-cross-section measurements for positrons and electrons colliding with H_2, N_2, and CO_2. *Phys. Rev. A* **1982**, *25*, 1393–1403. [CrossRef]
17. Zecca, A.; Chiari, L.; Sarkar, A.; Nixon, K.L.; Brunger, M.J. Total cross sections for positron scattering from H_2 at low energies. *Phys. Rev. A* **2009**, *80*, 032702. [CrossRef]
18. Machacek, J.R.; Anderson, E.K.; Makochekanwa, C.; Buckman, S.J.; Sullivan, J.P. Positron scattering from molecular hydrogen. *Phys. Rev. A* **2013**, *88*, 042715. [CrossRef]
19. Danby, G.; Tennyson, J. Differential cross sections for elastic positron-H_2 collisions using the R-matrix method. *J. Phys. B At. Mol. Opt. Phys.* **1990**, *23*, 1005–1016. [CrossRef]
20. Gibson, T.L. Low-energy positron-H_2 collisions in the distributed positron model. *J. Phys. B At. Mol. Opt. Phys.* **1992**, *25*, 1321–1336. [CrossRef]
21. Armour, E.A.G.; Baker, D.J.; Plummer, M. The theoretical treatment of low-energy e^+-H_2 scattering using the Kohn variational method. *J. Phys. B At. Mol. Opt. Phys.* **1990**, *23*, 3057–3074. [CrossRef]
22. Reid, D.D.; Klann, W.B.; Wadehra, J.M. Scattering of low-to intermediate-energy positrons from molecular hydrogen. *Phys. Rev. A* **2004**, *70*, 062714. [CrossRef]
23. Arretche, F.; Da Costa, R.; Sanchez, S.d.; Hisi, A.; De Oliveira, E.; Varella, M.D.N.; Lima, M. Similarities and differences in e±–molecule scattering: Applications of the Schwinger multichannel method. *Nucl. Instruments Methods Phys. Res. Sect. B Beam Interact. Mater. Atoms* **2006**, *247*, 13–19. [CrossRef]
24. Mukherjee, T.; Sarkar, N.K. Ro-vibrational close coupling study of positron–hydrogen molecule scattering using the parameter-free model correlation polarization potential. *J. Phys. B At. Mol. Opt. Phys.* **2008**, *41*, 125201. [CrossRef]
25. Gianturco, F.A.; Paioletti, P.; Rodriguez-Ruiz, J.A. Polarisation potentials for positron-molecule scattering processes. *Z. Phys. D Atoms Mol. Clust.* **1996**, *36*, 51–63. [CrossRef]
26. Zhang, R.; Baluja, K.L.; Franz, J.; Tennyson, J. Positron collisions with molecular hydrogen: Cross sections and annihilation parameters calculated using the *R*-Matrix Pseudo-States Method. *J. Phys. B At. Mol. Opt. Phys.* **2011**, *44*, 035203. [CrossRef]

27. Tenfen, W.; Mazon, K.T.; Michelin, S.E.; Arretche, F. Low-energy elastic positron cross sections for H_2 and N_2 using an Ab Initio Target Polariz. *Phys. Rev. A* **2012**, *86*, 042706. [CrossRef]
28. Zammit, M.C.; Fursa, D.V.; Bray, I. Convergent-close-coupling formalism for positron scattering from molecules. *Phys. Rev. A* **2013**, *87*, 020701. [CrossRef]
29. Zammit, M.C.; Fursa, D.V.; Savage, J.S.; Bray, I.; Chiari, L.; Zecca, A.; Brunger, M.J. Adiabatic-nuclei calculations of positron scattering from molecular hydrogen. *Phys. Rev. A* **2017**, *95*, 022707. [CrossRef]
30. Frighetto, F.F.; Barbosa, A.S.; Sanchez, S.d. Implementation of a model potential in the Schwinger multichannel method to describe polarization in positron-atom and -molecule scattering: Studies for the noble-gas atoms, H_2, and N_2. *Phys. Rev. A* **2023**, *108*, 012818. [CrossRef]
31. Kauppila, W.E.; Stein, T.S.; Smart, J.H.; Dababneh, M.S.; Ho, Y.K.; Downing, J.P.; Pol, V. Measurements of total scattering cross sections for intermediate-energy positrons and electrons colliding with helium, neon, and argon. *Phys. Rev. A* **1981**, *24*, 725–742. [CrossRef]
32. Charlton, M.; Humberston, J.W. *Positron Physics*, 1st ed.; Cambridge University Press: Cambridge, UK, 2000. [CrossRef]
33. Sullivan, J.P.; Makochekanwa, C.; Jones, A.; Caradonna, P.; Slaughter, D.S.; Machacek, J.; McEachran, R.P.; Mueller, D.W.; Buckman, S.J. Forward angle scattering effects in the measurement of total cross sections for positron scattering. *J. Phys. B At. Mol. Opt. Phys.* **2011**, *44*, 035201. [CrossRef]
34. Brunger, M.J.; Buckman, S.J.; Ratnavelu, K. Positron scattering from molecules: An experimental cross section compilation for positron transport studies and benchmarking theory. *J. Phys. Chem. Ref. Data* **2017**, *46*, 023102. [CrossRef]
35. Barp, M.V.; Tenfen, W.; Arretche, F. Many-body and single-body low-energy elastic positron scattering by beryllium atoms: From ab initio to semiempirical approaches. *Atoms* **2023**, *11*, 8. [CrossRef]
36. Zhang, J.Y.; Mitroy, J.; Varga, K. Positron scattering and annihilation from the hydrogen molecule at zero energy. *Phys. Rev. Lett.* **2009**, *103*, 223202. [CrossRef]
37. Zhang, J.Y.; Mitroy, J. Stochastic variational calculation of zero-energy positron scattering from H, He, and H_2. *Phys. Rev. A* **2011**, *83*, 022711. [CrossRef]
38. Tenfen, W.; Barp, M.V.; Arretche, F. Low-energy elastic scattering of positrons by O_2. *Phys. Rev. A* **2019**, *99*, 022703. [CrossRef]
39. Tenfen, W.; Seidel, E.P.; Barp, M.V.; Arretche, F. Higher order polarizabilities and the positron forward scattering problem: Convergence between calculated and measured cross sections in the very low energy regime. *J. Electron Spectrosc. Relat. Phenom.* **2022**, *255*, 147160. [CrossRef]
40. Gianturco, F.; Jain, A. The theory of electron scattering from polyatomic molecules. *Phys. Rep.* **1986**, *143*, 347–425. [CrossRef]
41. Stone, A. *The Theory of Intermolecular Forces*, 2nd ed.; Oxford University Press: Oxford, UK, 2013. [CrossRef]
42. Jain, A.; Gianturco, F.A. Low-energy positron collisions with CH_4 and SiH_4 molecules by using new positron polarization potentials. *J. Phys. B At. Mol. Opt. Phys.* **1991**, *24*, 2387–2398. [CrossRef]
43. Bransden, B.H.; Joachain, C.J. *Physics of Atoms and Molecules*, 1st ed.; Longman Scientific & Technical: Harlow, UK, 1990.
44. O'Connell, J.K.; Lane, N.F. Nonadjustable exchange-correlation model for electron scattering from closed-shell atoms and molecules. *Phys. Rev. A* **1983**, *27*, 1893–1903. [CrossRef]
45. Tenfen, W.; de Souza Glória, J.; Arretche, F. Low energy positron scattering by F and F_2. *J. Phys. Chem. A* **2022**, *126*, 7901–7915. [CrossRef]
46. Boroński, E.; Nieminen, R.M. Electron-positron density-functional theory. *Phys. Rev. B* **1986**, *34*, 3820–3831. [CrossRef]
47. Batsanov, S.S. Van der Waals radii of elements. *Inorg. Mater.* **2001**, *37*, 871–885. [CrossRef]
48. Ribeiro, E.; Machado, L.; Lee, M.T.; Brescansin, L. Application of the method of continued fractions to electron scattering by polyatomic molecules. *Comput. Phys. Commun.* **2001**, *136*, 117–125. [CrossRef]
49. Tenfen, W. Cálculo das Seções de Choque para Colisão de Pósitrons em Moléculas. Master's Thesis, Universidade Federal de Santa Catarina, Florianópolis, Brazil, 2009.
50. Arretche, F.; Tenfen, W.; Mazon, K.; Michelin, S.; Lima, M.; Lee, M.T.; Machado, L.; Fujimoto, M.; Pessoa, O. Low energy scattering of positrons by H_2O. *Nucl. Instruments Methods Phys. Res. Sect. B Beam Interact. Mater. Atoms* **2010**, *268*, 178–182. [CrossRef]
51. Machado, A.M.; Fujimoto, M.M.; Taveira, A.M.A.; Brescansin, L.M.; Lee, M.T. Application of the method of continued fractions to multichannel studies on electronic excitation of H_2 by electron impact. *Phys. Rev. A* **2001**, *63*, 032707. [CrossRef]
52. Nascimento, E.M.; Ribeiro, E.M.S.; Brescansin, L.M.; Lee, M.T.; Machado, L.E. Extension of the method of continued fractions to molecular photoionization: An application to ammonia. *J. Phys. B At. Mol. Opt. Phys.* **2003**, *36*, 3621–3627. [CrossRef]
53. Tenfen, W.; Arretche, F.; Michelin, S.; Mazon, K. Elastic and inelastic vibrational cross sections for positron scattering by carbon monoxide. *Nucl. Instruments Methods Phys. Res. Sect. B Beam Interact. Mater. Atoms* **2015**, *362*, 25–28. [CrossRef]
54. Barp, M.V.; Seidel, E.P.; Arretche, F.; Tenfen, W. Rotational excitation of N_2 by positron impact in the adiabatic rotational approximation. *J. Phys. B At. Mol. Opt. Phys.* **2018**, *51*, 205201. [CrossRef]
55. Huber, K.P.; Herzberg, G. *Molecular Spectra and Molecular Structure*; Constants of Diatomic Molecules; Springer: Boston, MA, USA, 1979; Volume IV. [CrossRef]

56. Maroulis, G.; Bishop, D.M. HF SCF electric polarizabilities and hyperpolarizabilities for the ground state of the hydrogen molecule. *Chem. Phys. Lett.* **1986**, *128*, 462–465. [CrossRef]
57. Dunning, T.H. Gaussian basis functions for use in molecular calculations. III. Contraction of (10s6p) atomic basis sets for the first-row atoms. *J. Chem. Phys.* **1971**, *55*, 716–723. [CrossRef]
58. Miliordos, E.; Hunt, K.L.C. Dependence of the multipole moments, static polarizabilities, and static hyperpolarizabilities of the hydrogen molecule on the H–H separation in the ground singlet state. *J. Chem. Phys.* **2018**, *149*, 234103. [CrossRef] [PubMed]
59. Dalgarno, A. Atomic polarizabilities and shielding factors. *Adv. Phys.* **1962**, *11*, 281–315. [CrossRef]
60. Buckingham, A.D. Permanent and Induced Molecular Moments and Long-Range Intermolecular Forces. In *Advances in Chemical Physics*, 1st ed.; Hirschfelder, J.O., Ed.; Wiley: New York, NY, USA, 1967; Volume 12, pp. 107–142. [CrossRef]
61. Thakkar, A.J.; Lupinetti, C. Atomic Polarizabilities and Hyperpolarizabilities: A Critical Compilation. In *Atoms, Molecules and Clusters in Electric Fields*; World Scientific Publishing Co.: Hackensack, NJ, USA, 2006; pp. 505–529. [CrossRef]
62. Maroulis, G.; Thakkar, A.J. Multipole moments, polarizabilities, and hyperpolarizabilities for N_2 from fourth-order many-body perturbation theory calculations. *J. Chem. Phys.* **1988**, *88*, 7623–7632. [CrossRef]
63. O'Malley, T.F. Extrapolation of electron-rare gas atom cross sections to zero energy. *Phys. Rev.* **1963**, *130*, 1020–1029. [CrossRef]
64. Thompson, D.G. The elastic scattering of slow electrons by neon and argon. *Proc. R. Soc. London. Ser. A. Math. Phys. Sci.* **1966**, *294*, 160–174. [CrossRef]
65. Sullivan, J.; Gilbert, S.; Marler, J.; Barnes, L.; Buckman, S.; Surko, C. Low energy positron scattering and annihilation studies using a high resolution trap-based beam. *Nucl. Instruments Methods Phys. Res. Sect. B Beam Interact. Mater. Atoms* **2002**, *192*, 3–16. [CrossRef]
66. Zecca, A.; Chiari, L.; Sarkar, A.; Brunger, M.J. Positron scattering from the isoelectronic molecules N_2, CO and C_2H_2. *New J. Phys.* **2011**, *13*, 115001. [CrossRef]
67. Seidel, E.P.; Arretche, F. Rearrangement collisions in the Schwinger variational principle: A long-standing problem in positron scattering physics. *J. Phys. Chem. Lett.* **2023**, *14*, 2263–2267. [CrossRef] [PubMed]
68. Fedus, K.; Franz, J.; Karwasz, G.P. Positron scattering on molecular hydrogen: Analysis of experimental and theoretical uncertainties. *Phys. Rev. A* **2015**, *91*, 062701. [CrossRef]
69. Cheong, Z.; Stevens, D.; Sullivan, J.P. Positron scattering from ethane: Elastic and inelastic scattering. *Phys. Rev. A* **2024**, *110*, 022815. [CrossRef]
70. Machacek, J.R.; McEachran, R.P. Partial wave analysis for folded differential cross sections. *J. Phys. B At. Mol. Opt. Phys.* **2018**, *51*, 065007. [CrossRef]
71. Cheong, Z.; Babij, T.J.; Anthouard, B.; Machachek, J.R.; McEachran, R.P.; Sullivan, J.P. Elastic scattering and electronic excitation in positron interactions with neon. *J. Phys. B At. Mol. Opt. Phys.* **2021**, *54*, 065204. [CrossRef]
72. Pinheiro, J.G.; Assafrão, D.; Poveda, L.A.; Mohallem, J.R. Elastic and inelastic cross sections for positron scattering from molecular oxygen. *Eur. Phys. J. D* **2023**, *77*, 184. [CrossRef]
73. Karwasz, G.; Pliszka, D.; Brusa, R. Total cross sections for positron scattering in argon, nitrogen and hydrogen below 20eV. *Nucl. Instruments Methods Phys. Res. Sect. B Beam Interact. Mater. Atoms* **2006**, *247*, 68–74. [CrossRef]
74. Swann, A.R.; Gribakin, G.F. Model-potential calculations of positron binding, scattering, and annihilation for atoms and small molecules using a Gaussian basis. *Phys. Rev. A* **2020**, *101*, 022702. [CrossRef]